Chapter 4

A robust adaptive numerical method for singularly perturbed delay parabolic problems with Robin boundary conditions

In this chapter, we consider a singularly perturbed parabolic reaction-diffusion equation with time delay. We define the model problem as follows

$$\mathcal{L}y \coloneqq \frac{\partial y}{\partial t} + \mathcal{L}_\varepsilon y = f(x,t) - b(x,t)y(x,t-\tau),\ (x,t) \in (0,1)\times(0,T], \tag{4.1}$$

with the initial condition in time

$$y(x,t) = \phi_b(x,t),\ (x,t) \in [0,1]\times[-\tau,0], \tag{4.2}$$

and the Robin boundary conditions in space

$$\begin{cases} \mathcal{D}_0 y(0,t) \coloneqq y(0,t) - \sqrt{\varepsilon}\frac{\partial y}{\partial x}(0,t) = \phi_0(t),\ t \in (0,T], \\ \mathcal{D}_1 y(1,t) \coloneqq y(1,t) + \sqrt{\varepsilon}\frac{\partial y}{\partial x}(1,t) = \phi_1(t),\ t \in (0,T], \end{cases} \tag{4.3}$$

where $\mathcal{L}_\varepsilon y \coloneqq -\varepsilon\frac{\partial^2 y}{\partial x^2} + a(x,t)y$, and $0 < \varepsilon \leq 1$ and $\tau > 0$ define the singular perturbation parameter and the constant delay in the solution input, respectively. In addition, we consider $0 < \alpha \leq a(x,t)$ and $0 < \beta \leq b(x,t)$ in $[0,1]\times[0,T]$ for some constants α and β, which ensures the maximum principle for the operator $\mathcal{L}$.

The existence and uniqueness of the solution can be confirmed from [98, Theorem 4] under sufficient smoothness of the input functions.

Some examples of singularly perturbed delay differential equations are found in population dynamics [126], variational problems in control theory [127], study of bistable devices [128], explanation of human pupil–light reflex [129], tumor growth and neural networks [130]. In these models, the time delay factor includes some previous behavior which helps to model the phenomena more practically. For example, in population ecology the hatching period or gestation period is represented by the delay term, in control systems the delay term appears because of the finite speed of the controller and some other important examples of delay differential singular perturbation problems can be found in [91].

The presence of the delay term in the differential equation and the Robin boundary conditions indeed make the theoretical part little complicated, due to which problem (4.1)-(4.3) is less studied in the literature. In the present chapter, our main motive is to construct a high order parameter-robust numerical method for the time-delayed reaction-diffusion problems with Robin boundary conditions using layer-adaptive equidistribution meshes. Since, meshes are moving at every time step, we have to use a modified version of Euler scheme in time. The moving mesh algorithm requires discretization of the problem and the discretization of a suitable error monitor function. Here, we consider a special discretization for Robin boundary conditions which will make the convergence, quadratic in space. To simplify the convergence analysis, we assume T is divisible by τ. Next, we provide the convergence analysis and prove that the present approach is first order accurate in time and second order accurate in space. The validity and effectiveness of the present method is also shown through some numerical experiments.

This chapter is structured as follows: In Section 4.1, we provide some properties of the solution of problem (4.1)-(4.3). A finite difference discretization of the problem and the formation of adaptive mesh is given in Section 4.2. Section 4.3 is completely devoted to the error analysis for the proposed method. In Section 4.4, the numerical results for two test examples are given and discussed. Then, the chapter concludes with Section 4.5.

4.1 Properties of the continuous problem

The continuous problem (4.1) satisfies the following maximum principle which is useful for obtaining the uniform stability of the continuous solution.

Theorem 4.1.1. [98](Continuous maximum principle) Assume that the function z satisfies $\mathcal{L}z \geq 0$, for $(x,t) \in (0,1] \times (0,T]$, $\mathcal{D}_0 z(0,t) \geq 0$ for $t \in (0,T]$, $\mathcal{D}_1 z(1,t) \geq 0$ for $t \in (0,T]$ and $z(x,0) \geq 0$ for $x \in [0,1]$. Then $z(x,t) \geq 0$ for $(x,t) \in [0,1] \times [0,T]$.

The following uniform stability estimate holds for the continuous problem (4.1).

Corollary 4.1.1. [98] The solution y of (4.1) satisfies the following bound

$$\|y\|_{[0,1]\times[0,T]} \leq \max\left\{\frac{1}{\alpha}\|\mathcal{L}y\|_{[0,1]\times[0,T]}, \|\mathcal{D}_0 y\|_{\{0\}\times[0,T]}, \|\mathcal{D}_1 y\|_{\{1\}\times[0,T]}, \|y\|_{[0,1]\times[-\tau,0]}\right\}.$$

We now describe a suitable solution decomposition which will help us to prove the convergence analysis of our proposed method. Based on the method of steps, we partition the time interval $[0,T]$ by using delay term τ, such as $[0,\tau]$, $[\tau,2\tau]$ and so on, so that we can decompose the convergence analysis on each partition separately. Note that in $[0,\tau]$, the right hand side, $f - b\phi_b(x,t-\tau)$ is independent of ε. Hence,

for $t \in [0, \tau]$, (4.1)-(4.3) can be written as

$$\mathcal{L}y = f - b\phi_b(x, t-\tau), \quad (x,t) \in (0,1) \times (0,\tau], \tag{4.4}$$

$$\text{with} \quad y(x,0) = \phi_b(x,0),\ x \in [0,1], \quad \text{and} \quad \begin{cases} \mathcal{D}_0 y(0,t) = \phi_0(t),\ t \in (0,\tau], \\ \mathcal{D}_1 y(1,t) = \phi_1(t),\ t \in (0,\tau]. \end{cases}$$

Now, we decompose the solution y into smooth and singular components s and w, resp., so that $y = s + w$ and smooth component's derivatives are uniformly bounded upto certain order. To derive this, the smooth component is further decomposed as $s = s_0 + \varepsilon s_1$, so that s_0 and s_1 satisfy the following problems

$$\frac{\partial s_0}{\partial t}(x,t) + a s_0(x,t) = f - b\phi_b(x, t-\tau), \quad (x,t) \in (0,1) \times (0,\tau], \tag{4.5}$$

$$\text{with} \quad s_0(x,0) = \phi_b(x,0),\ x \in [0,1],$$

and

$$\mathcal{L}s_1 = \frac{\partial^2 s_0}{\partial x^2}(x,t), \quad (x,t) \in (0,1) \times (0,\tau], \tag{4.6}$$

$$\text{with} \quad s_1(x,0) = 0,\ x \in [0,1], \quad \text{and} \quad \begin{cases} \mathcal{D}_0 s_1(0,t) = 0,\ t \in (0,\tau], \\ \mathcal{D}_1 s_1(1,t) = 0,\ t \in (0,\tau], \end{cases}$$

respectively. Thus, the smooth component s satisfies

$$\mathcal{L}s = f(x,t) - b\phi_b(x, t-\tau), \quad (x,t) \in (0,1) \times (0,\tau], \tag{4.7}$$

$$\text{with} \quad s(x,0) = \phi_b(x,0),\ x \in [0,1], \quad \text{and} \quad \begin{cases} \mathcal{D}_0 s(0,t) = \mathcal{D}_0 s_0(0,t),\ t \in (0,\tau], \\ \mathcal{D}_1 s(1,t) = \mathcal{D}_1 s_0(1,t),\ t \in (0,\tau], \end{cases}$$

and the singular component w is determined by the following problem

$$\mathcal{L}w = 0, \quad (x,t) \in (0,1) \times (0,\tau], \tag{4.8}$$

with $w(x,0)=0,\ x\in[0,1]$, and $\begin{cases}\mathcal{D}_0 w(0,t)=\phi_0(t)-\mathcal{D}_0 s_0(0,t),\ t\in(0,\tau],\\ \mathcal{D}_1 w(1,t)=\phi_1(t)-\mathcal{D}_1 s_0(1,t),\ t\in(0,\tau].\end{cases}$

Now we break the singular component into left and right layer parts so that $w = w_{ll}+w_{rr}$, where the left component w_{ll} is computed by

$$\mathcal{L}w_{ll}=0,\quad (x,t)\in(0,1)\times(0,\tau], \tag{4.9}$$

with $w_{ll}(x,0)=0,\ x\in[0,1]$, and $\begin{cases}\mathcal{D}_0 w_{ll}(0,t)=\phi_0(t)-\mathcal{D}_0 s_0(0,t),\ t\in(0,\tau],\\ \mathcal{D}_1 w_{ll}(1,t)=0,\ t\in(0,\tau],\end{cases}$

and the right component w_{rr} is computed by

$$\mathcal{L}w_{rr}=0,\quad (x,t)\in(0,1)\times(0,\tau],$$

with $w_{rr}(x,0)=0,\ x\in[0,1]$ and $\begin{cases}\mathcal{D}_0 w_{rr}(0,t)=0,\ t\in(0,\tau],\\ \mathcal{D}_1 w_{rr}(1,t)=\phi_1(t)-\mathcal{D}_1 s_0(1,t),\ t\in(0,\tau].\end{cases}$

Now, for $t\in[\tau,2\tau]$, we write (4.1)-(4.3) as

$$\mathcal{L}y=f-by(x,t-\tau),\quad (x,t)\in(0,1)\times(\tau,2\tau], \tag{4.10}$$

with $y(x,t)=y(x,t),\ (x,t)\in[0,1]\times[0,\tau]$, and $\begin{cases}\mathcal{D}_0 y(0,t)=\phi_0(t),\ t\in(\tau,2\tau],\\ \mathcal{D}_1 y(1,t)=\phi_1(t),\ t\in(\tau,2\tau].\end{cases}$

Again we decompose the solution y into smooth and singular components as $y = s+w$. The smooth component s is further decomposed as $s=s_0+\varepsilon s_1$, where s_0 and s_1 respectively, satisfy the following problems

$$\frac{\partial s_0}{\partial t}(x,t)+as_0(x,t)=f-bs_0(x,t-\tau),\quad (x,t)\in(0,1)\times(\tau,2\tau], \tag{4.11}$$

$$\text{with} \quad s_0(x,t) = y(x,t),\ (x,t) \in [0,1] \times [0,\tau],$$

and

$$\mathcal{L}s_1 = -bs_1(x,t-\tau) + \frac{\partial^2 s_0}{\partial x^2}(x,t), \quad (x,t) \in (0,1) \times (\tau, 2\tau],$$

$$\text{with} \quad s_1(x,t) = 0,\ (x,t) \in [0,1] \times [0,\tau], \quad \text{and} \quad \begin{cases} \mathcal{D}_0 s_1(0,t) = 0,\ t \in (\tau, 2\tau], \\ \mathcal{D}_1 s_1(1,t) = 0,\ t \in (\tau, 2\tau]. \end{cases}$$

Thus, the smooth component s satisfies

$$\mathcal{L}s = f(x,t) - bs(x,t-\tau), \quad (x,t) \in (0,1) \times (\tau, 2\tau], \tag{4.12}$$

$$\text{with} \quad s(x,t) = y(x,t),\ (x,t) \in [0,1] \times [0,\tau],$$

$$\text{and} \quad \begin{cases} \mathcal{D}_0 s(0,t) = \mathcal{D}_0 s_0(0,t),\ t \in (\tau, 2\tau], \\ \mathcal{D}_1 s(1,t) = \mathcal{D}_1 s_0(1,t),\ t \in (\tau, 2\tau], \end{cases}$$

and the singular component w is determined by

$$\mathcal{L}w = -bw(x,t-\tau), \quad (x,t) \in (0,1) \times (\tau, 2\tau], \tag{4.13}$$

$$\text{with} \quad w(x,t) = 0,\ (x,t) \in [0,1] \times [0,\tau],$$

$$\text{and} \quad \begin{cases} \mathcal{D}_0 w(0,t) = \phi_0(t) - \mathcal{D}_0 s_0(0,t),\ t \in (\tau, 2\tau], \\ \mathcal{D}_1 w(1,t) = \phi_1(t) - \mathcal{D}_1 s_0(1,t),\ t \in (\tau, 2\tau]. \end{cases}$$

Similar to the interval $[0,\tau]$, we break the singular component in left and right parts as $w = w_{ll} + w_{rr}$, where the left part w_{ll} is obtained by

$$\mathcal{L}w_{ll} = -bw_{ll}(x,t-\tau), \quad (x,t) \in (0,1) \times (\tau, 2\tau], \tag{4.14}$$

$$\text{with} \quad w_{ll}(x,t) = 0,\ (x,t) \in [0,1] \times [0,\tau],$$

$$\text{and} \quad \begin{cases} \mathcal{D}_0 w_{ll}(0,t) = \phi_0(t) - \mathcal{D}_0 s_0(0,t), \ t \in (\tau, 2\tau], \\ \mathcal{D}_1 w_{ll}(1,t) = 0, \ t \in (\tau, 2\tau], \end{cases}$$

and the right part w_{rr} is obtained by

$$\mathcal{L} w_{rr} = -b w_{rr}(x, t-\tau), \quad (x,t) \in (0,1) \times (\tau, 2\tau], \tag{4.15}$$

$$\text{with} \quad w_{rr}(x,t) = 0, \ (x,t) \in [0,1] \times [0,\tau],$$

$$\text{and} \quad \begin{cases} \mathcal{D}_0 w_{rr}(0,t) = 0, \ t \in (\tau, 2\tau], \\ \mathcal{D}_1 w_{rr}(1,t) = \phi_1(t) - \mathcal{D}_1 s_0(1,t), \ t \in (\tau, 2\tau]. \end{cases}$$

In an analogous way, we extend the decomposition approaches at each partitions to get the decomposition on $[0,T]$. Now, we can use the arguments given in [98], to obtain the following result.

Theorem 4.1.2. The decomposition $y = s + w_{ll} + w_{rr}$ of (4.1)-(4.3) satisfies the following bounds

$$\left\| \frac{\partial^{p+q} s}{\partial x^p \partial t^q} \right\|_{[0,1]\times[0,T]} \leq C(1 + \varepsilon^{1-p/2}), \tag{4.16}$$

$$\left| \frac{\partial^{p+q} w_{ll}}{\partial x^p \partial t^q} \right| \leq C \varepsilon^{-\frac{p}{2}} e^{-\frac{x}{\sqrt{\varepsilon}}}, \tag{4.17}$$

$$\left| \frac{\partial^{p+q} w_{rr}}{\partial x^p \partial t^q} \right| \leq C \varepsilon^{-\frac{p}{2}} e^{-\frac{(1-x)}{\sqrt{\varepsilon}}}, \quad 1 \leq p + 2q \leq 4, \ p, q \in \mathbb{N}_0, (x,t) \in [0,1] \times [0,T]. \tag{4.18}$$

4.2 Discretization and mesh generation

4.2.1 The discrete problem

From Theorem 4.1.2, it can be observed that the boundary layer is not varying with respect to time. Hence, we take a uniform mesh with total number of mesh points

M for partitioning the time interval $[0,T]$. In addition, we divide this domain in m sub-intervals of equal length τ so that $M = mM_\tau$. Hence, each of these sub-intervals is now divided in M_τ equal mesh-elements with time step-size $\Delta t = \tau/M_\tau$. We also divide $[-\tau, 0]$ into M_τ equal mesh-elements. On each time t_j, a non-uniform mesh $\{x_i^j\}_{i=0}^N$ is considered in the spatial direction with step size $h_i^j = x_i^j - x_{i-1}^j$, $i = 1, \ldots, N$. Thus, the discretization of the domain is the tensor product of these two 1D space-time meshes. On this discrete domain, (4.1) is discretized as follows

$$L^{N,M}Y_i^j := \delta_t^\star Y_i^j + L_\varepsilon^{N,M} Y_i^j = f_i^j - b_i^j \widetilde{Y}_i^{j-M_\tau}, \quad i = 1, ..., N-1,\ j = 1, ..., M, \tag{4.19}$$

with the discretized initial and boundary conditions

$$Y_i^j = (\phi_b)_i^j, \quad i = 0, ..., N,\ j = -M_\tau, ..., 0, \tag{4.20}$$

and

$$\begin{cases} D_0^{N,M}Y_0^j := Y_0^j - \sqrt{\varepsilon} D_x^+ Y_0^j + \frac{h_1^j}{2\sqrt{\varepsilon}}(a_0^j Y_0^j + \delta_t^\star Y_0^j) \\ \qquad\qquad = (\phi_0)_0^j + \frac{h_1^j}{2\sqrt{\varepsilon}}\left(f_0^j - b_0^j \widetilde{Y}_0^{j-M_\tau}\right), \quad j = 1, ..., M, \\ D_1^{N,M}Y_N^j = Y_N^j + \sqrt{\varepsilon} D_x^- Y_N^j + \frac{h_N^j}{2\sqrt{\varepsilon}}(a_N^j Y_N^j + \delta_t^\star Y_N^j) \\ \qquad\qquad = (\phi_1)_N^j + \frac{h_N^j}{2\sqrt{\varepsilon}}\left(f_N^j - b_N^j \widetilde{Y}_N^{j-M_\tau}\right), \quad j = 1, ..., M, \end{cases} \tag{4.21}$$

where

$$L_\varepsilon^{N,M} Y_i^j = -\varepsilon \delta_x^2 Y_i^j + a_i^j Y_i^j, \quad \delta_t^\star Y_i^j = \frac{Y_i^j - \widetilde{Y}_i^{j-1}}{\Delta t},$$

$$D_x^+ Y_i^j = \frac{Y_{i+1}^j - Y_i^j}{h_{i+1}^j}, \quad D_x^- Y_i^j = \frac{Y_i^j - Y_{i-1}^j}{h_i^j}, \quad \delta_x^2 Y_i^j = \frac{(D_x^+ - D_x^-)Y_i^j}{(h_i^j + h_{i+1}^j)/2}.$$

Here, $\widetilde{Y}_i^{j-1}$ and $\widetilde{Y}_i^{j-M_\tau}$ represent the linear interpolants of Y_i^{j-1} and $Y_i^{j-M_\tau}$, respectively, at the spatial mesh points x_i^j. The discretization satisfies the following discrete maximum principle which can be obtained by following the arguments, given in [98].

Lemma 4.2.1. Consider a mesh function U such that $L^{N,M}U_i^j \geq 0$, for $i = 1, ..., N-1,\ j = 1, ..., M,\ D_0^{N,M}U_0^j \geq 0,\ D_1^{N,M}U_N^j \geq 0$ for $j = 1, ..., M$ and $U_i^j \geq 0,\ i = 1, ..., N,\ j = 0$. Then $U_i^j \geq 0$, for $i = 0, ..., N,\ j = 0, ..., M$.

From the above lemma, we also get the stability of the discrete solution.

4.2.2 Mesh equidistribution

We construct the adaptive mesh in the spatial direction based on the equidistribution principle [47, 65, 131]. At any time level t_k, the equidistributed mesh $\{x_i^k\}$ is obtained by the following equidistribution principle

$$\int_{x_{i-1}^k}^{x_i^k} \mathcal{M}(y(\gamma, t_k), \gamma)d\gamma = \frac{1}{N}\int_0^1 \mathcal{M}(y(\gamma, t_k), \gamma)d\gamma, \quad i = 1, ..., N, \tag{4.22}$$

where $\mathcal{M}(y(x, t_k), x) > 0$ is called the monitor function. This principle can also be formulated as follows:

$$\int_0^{x^k(\xi)} \mathcal{M}(y(\gamma, t_k), \gamma)d\gamma = \xi\int_0^1 \mathcal{M}(y(\gamma, t_k), \gamma)d\gamma, \tag{4.23}$$

where (4.22) is formulated as an invertible mapping from the computational uniform coordinates $\xi \in [0, 1]$ to the physical non-uniform coordinates $x^k \in [0, 1]$.

In the literature, several type of monitor functions are available, based on the problem being considered and the discretization being used. In the present research, we consider a monitor function constituting the second derivative of the singular component of the solution and a positive constant $\aleph^k$, independent of N, (motivated from [56]). The choice of singular component will make our analysis simpler. In practice, this component can be replaced by the solution, itself. The positive constant $\aleph^k$ is chosen to prevent mesh starvation in the regular part of the solution and

to improve the robustness of the adaptive mesh. Here, we consider the following monitor function

$$\mathcal{M}(y(x,t_k),x) = \aleph^k + \left|\frac{\partial^2 w}{\partial x^2}(x,t_k)\right|^{1/2}, \tag{4.24}$$

where $\aleph^k$ can be chosen according to Lemma 4.2.2 given later.

Now we check the mesh structure generated by the equidistribution of the monitor function (4.24). Let us use the approximation

$$\left|\frac{\partial^2 w}{\partial x^2}(x,t_k)\right|^{1/2} \approx |\nu_1|^{1/2}\varepsilon^{-1/2}e^{-\frac{x}{2\sqrt{\varepsilon}}} + |\nu_2|^{1/2}\varepsilon^{-1/2}e^{-\frac{(1-x)}{2\sqrt{\varepsilon}}}, \quad x\in[0,1], \tag{4.25}$$

where ν_1 and ν_2 are the constants independent of ε and x. Thus,

$$\int_0^1 \left|\frac{\partial^2 w}{\partial s^2}(s,t_k)\right|^{1/2} ds \approx 2(|\nu_1|^{1/2}+|\nu_2|^{1/2})(1-e^{-\frac{1}{2\sqrt{\varepsilon}}}) := \mathbf{K}.$$

Using the approximation (4.25) in the monitor function (4.24), the equidistribution principle (4.23) leads to the following mapping

$$\xi\left(\frac{\aleph^k}{\mathbf{K}}+1\right) = \frac{\aleph^k}{\mathbf{K}}x^k(\xi) + \lambda_1\left(1-e^{-\frac{x^k(\xi)}{2\sqrt{\varepsilon}}}\right) + \lambda_2\left(e^{-\frac{(1-x^k(\xi))}{2\sqrt{\varepsilon}}} - e^{-\frac{1}{2\sqrt{\varepsilon}}}\right), \tag{4.26}$$

where

$$\lambda_1 = \frac{|\nu_1|^{1/2}}{(|\nu_1|^{1/2}+|\nu_2|^{1/2})(1-e^{-\frac{1}{2\sqrt{\varepsilon}}})} \quad \text{and} \quad \lambda_2 = \frac{|\nu_2|^{1/2}}{(|\nu_1|^{1/2}+|\nu|_2^{1/2})(1-e^{-\frac{1}{2\sqrt{\varepsilon}}})}.$$

Note that $0\le\lambda_1,\lambda_2\le 1+\mathcal{O}(e^{-1/\sqrt{\varepsilon}})$. Hence, the uniform mesh $\{\xi_i = i/N\}_{i=0}^N$ on the computational domain is mapped to a non-uniform equidistributed mesh $\{x_i^k\}_{i=0}^N$ on the physical domain by the following way

$$\frac{i}{N}\left(\frac{\aleph^k}{\mathbf{K}}+1\right) = \frac{\aleph^k}{\mathbf{K}}x_i^k + \lambda_1\left(1-e^{-\frac{x_i^k}{2\sqrt{\varepsilon}}}\right) + \lambda_2\left(e^{-\frac{(1-x_i^k)}{2\sqrt{\varepsilon}}} - e^{-\frac{1}{2\sqrt{\varepsilon}}}\right). \tag{4.27}$$

Lemma 4.2.2. Assuming $\aleph^k = \mathbf{K}$, the equidistributed mesh obtained from (4.27) satisfies

$$x^k_{\mathcal{S}} < 2\sqrt{\varepsilon}\ln(N) < x^k_{\mathcal{S}+1} \quad \text{and} \quad x^k_{\wp-1} < 1 - 2\sqrt{\varepsilon}\ln(N) < x^k_{\wp},$$

where

$$\mathcal{S} = \left[\frac{1}{2}\left(2\sqrt{\varepsilon}N\ln(N) + \lambda_1(N-1) + \lambda_2 N(N-1)e^{-\frac{1}{2\sqrt{\varepsilon}}}\right)\right],$$

$$\wp = \left[N - \frac{1}{2}\left(2\sqrt{\varepsilon}N\ln(N) + \lambda_1 N(N-1)e^{-\frac{1}{2\sqrt{\varepsilon}}} + \lambda_2(N-1)\right)\right] + 1,$$

and $[\cdot]$ is the integer part of the value. Moreover, the mesh spacing for $i = 1, ..., \mathcal{S}$ and for $i = \wp + 1, ..., N$ satisfies $h^k_i < C\sqrt{\varepsilon}$ with

$$|h^k_{i+1} - h^k_i| \le C(h^k_i)^2,\ i = 1, 2, \ldots, \mathcal{S} - 1,$$

$$\text{and}\ \ |h^k_{i+1} - h^k_i| \le C(h^k_{i+1})^2,\ i = \wp + 1, ..., N - 1.$$

Further, we have

$$e^{-\frac{x^k_i}{2\sqrt{\varepsilon}}} \le CN^{-1} \text{ for } i \ge \mathcal{S} - 1, \quad \text{and} \quad e^{-\frac{(1-x^k_i)}{2\sqrt{\varepsilon}}} \le CN^{-1} \text{ for } i \le \wp + 1.$$

Proof. It can be easily observed that there must exist two positive integers $\mathcal{S}$ and $\wp$ such that $x^k_{\mathcal{S}} < 2\sqrt{\varepsilon}\ln(N) < x^k_{\mathcal{S}+1}$ and $x^k_{\wp-1} < 1 - 2\sqrt{\varepsilon}\ln(N) < x^k_{\wp}$ respectively, since, $0 < 2\sqrt{\varepsilon}\ln(N) < 1$ and also $0 < 1 - 2\sqrt{\varepsilon}\ln(N) < 1$, are true, for sufficiently small ε.

By substituting $x^k_i = 2\sqrt{\varepsilon}\ln(N)$ in (4.27) and considering $\aleph^k = \mathbf{K}$, the value of $\mathcal{S}$ follows by solving for i. The procedure for obtaining $\wp$ is analogous.

To prove the bound on mesh spacing for $i = 1, ..., \mathcal{S} - 1$, we find upper and lower bounds of the position of mesh points x^k_i. Taking $\aleph^k = \mathbf{K}$ and noting that

$\left(e^{-\frac{(1-\overline{x}_i^k)}{2\sqrt{\varepsilon}}} - e^{-\frac{1}{2\sqrt{\varepsilon}}}\right) = \mathcal{O}(e^{-1/\sqrt{\varepsilon}})$, from (4.27) we get $x_i^k < \overline{x}^k$, where

$$\frac{2i}{\lambda_1 N} = \left(1 - e^{-\frac{\overline{x}_i^k}{2\sqrt{\varepsilon}}}\right).$$

Hence

$$\overline{x}_i^k = -2\sqrt{\varepsilon}\ln\left(1 - \frac{2i}{\lambda_1 N}\right). \tag{4.28}$$

Now using this upper bound in (4.27) we have $x_i^k > \underline{x}_i^k$, where

$$\underline{x}_i^k = -2\sqrt{\varepsilon}\ln\left(1 - \frac{1}{\lambda_1}\left(\frac{2i}{N} + 2\sqrt{\varepsilon}\ln\left(1 - \frac{2i}{\lambda_1 N}\right)\right)\right). \tag{4.29}$$

Thus, from equations (4.28) and (4.29), we have

$$\begin{aligned} h_i^k < \overline{x}_i^k - \underline{x}_{i-1}^k &= 2\sqrt{\varepsilon}\ln\left(1 + \frac{2 + 2\sqrt{\varepsilon}N\ln\left(\lambda_1 N/(\lambda_1 N - 2(i-1))\right)}{\lambda_1 N - 2i}\right) \\ &< C\sqrt{\varepsilon}. \end{aligned}$$

Similarly we can prove the result for $i = \wp + 1, ..., N - 1$.

Now taking $\aleph^k = \mathbf{K}$ and noting that $\left(e^{-\frac{(1-\overline{x}_i^k)}{2\sqrt{\varepsilon}}} - e^{-\frac{1}{2\sqrt{\varepsilon}}}\right) = \mathcal{O}(e^{-1/\sqrt{\varepsilon}})$, from (4.27), we have

$$\begin{aligned} e^{-\frac{x_{\mathcal{S}-1}^k}{2\sqrt{\varepsilon}}} &= \frac{1}{\lambda_1}\left(\lambda_1 + x_{\mathcal{S}-1} - \frac{2(\mathcal{S}-1)}{N}\right) \\ &\leq \frac{1}{\lambda_1}\Bigg(\lambda_1 + 2\sqrt{\varepsilon}\ln(N) - \frac{1}{N}\Big[2\sqrt{\varepsilon}N\ln(N) + \lambda_1(N-1) \\ &\qquad + \lambda_2 N(N-1)e^{-\frac{1}{2\sqrt{\varepsilon}}} - 2\Big]\Bigg) \\ &\leq CN^{-1}. \end{aligned}$$

Thus, for $i \geq \mathcal{S} - 1$, we obtain $e^{-\frac{x_{\mathcal{S}-1}^k}{2\sqrt{\varepsilon}}} \leq CN^{-1}$. A similar proof can be done for $i \leq \wp + 1$.

□

Lemma 4.2.3. For $i = 1, ..., N$, the mesh spacing satisfies

$$h_i^k \leq CN^{-1}.$$

Proof. The proof is a direct consequence of the equidistribution principle (4.22) and the choice $\aleph^k = \mathbf{K}$, cf. Lemma 3.16. □

4.3 Error analysis

In this section, we discuss the convergence analysis of the proposed method on equidistributed meshes. The main result is proved in the following theorem.

Theorem 4.3.1. Let $y(x_i^j, t_j)$ and Y_i^j be the solutions of (4.1)-(4.3) and (4.19)-(4.21), respectively. If for some $0 < \rho < 1$, $N^{-\rho} \leq C\Delta t$, then we have the following estimate

$$|y(x_i^j, t_j) - Y_i^j| \leq C(\Delta t + N^{-2+\rho}) \quad \text{for all } i = 0, \ldots, N,\ j = 0, \ldots, M.$$

Proof. For $t_j \in [0, \tau]$, we have

$$L^{N,M} Y_i^j = f_i^j - b_i^j (\phi_b)_i^{j-M_\tau}, \quad i = 1, ..., N-1,\ j = 1, ..., M_\tau, \tag{4.30}$$

$$\text{with} \quad Y_i^0 = (\phi_b)_i^0, \quad i = 0, ..., N,$$

$$\text{and} \quad \begin{cases} D_0^{N,M} Y_0^j = \phi_0(t_j) + \frac{h_1^j}{2\sqrt{\varepsilon}} \left(f_0^j - b_0^j (\phi_b)_0^{j-M_\tau} \right), & j = 1, ..., M_\tau, \\ D_1^{N,M} Y_N^j = \phi_1(t_j) + \frac{h_N^j}{2\sqrt{\varepsilon}} \left(f_N^j - b_N^j (\phi_b)_N^{j-M_\tau} \right), & j = 1, ..., M_\tau. \end{cases}$$

Analogous to the decomposition of y of (4.4), we consider the decomposition of discrete solution Y as $Y = S + W$, where S satisfies the following discrete problem

$$L^{N,M} S_i^j = f_i^j - b_i^j (\phi_b)_i^{j-M_\tau}, \quad i = 1, ..., N-1, \ j = 1, ..., M_\tau, \tag{4.31}$$

$$\text{with} \quad S_i^0 = (\phi_b)_i^0, \quad i = 0, ..., N,$$

$$\text{and} \quad \begin{cases} D_0^{N,M} S_0^j = \mathcal{D}_0 s(0, t_j) + \frac{h_1^j}{2\sqrt{\varepsilon}} \left(f_0^j - b_0^j (\phi_b)_0^{j-M_\tau} \right), \quad j = 1, ..., M_\tau, \\ D_1^{N,M} S_N^j = \mathcal{D}_1 s(1, t_j) + \frac{h_N^j}{2\sqrt{\varepsilon}} \left(f_N^j - b_N^j (\phi_b)_N^{j-M_\tau} \right), \quad j = 1, ..., M_\tau, \end{cases}$$

and W is the solution of the following discrete problem

$$L^{N,M} W_i^j = 0, \quad i = 1, ..., N-1, \ j = 1, ..., M_\tau, \tag{4.32}$$

$$\text{with} \quad W_i^0 = 0, \quad i = 0, ..., N,$$

$$\text{and} \quad \begin{cases} D_0^{N,M} W_0^j = \phi_0(t_j) - \mathcal{D}_0 s(0, t_j), \quad j = 1, ..., M_\tau, \\ D_1^{N,M} W_N^j = \phi_1(t_j) - \mathcal{D}_1 s(1, t_j), \quad j = 1, ..., M_\tau. \end{cases}$$

Then the error can be decomposed as

$$|y - Y| \leq |s - S| + |w - W|. \tag{4.33}$$

Hence, we can estimate the errors in smooth and singular components separately. First, to estimate the truncation error for the smooth component, using the continuous problem (4.7) and the discrete problem (4.31), we have

$$[L^{N,M}(s - S)]_i^j = -\varepsilon \left(\delta_x^2 - \frac{\partial^2}{\partial x^2} \right) s(x_i^j, t_j) + \left(\delta_t^\star - \frac{\partial}{\partial t} \right) s(x_i^j, t_j).$$

Now we use Taylor expansion with standard interpolation error estimate, and the condition $N^{-\rho} \leq C\Delta t$ for some $0 < \rho < 1$ and obtain

$$|[L^{N,M}(s-S)]_i^j| \leq \max_{\eta\in[x_{i-1}^j, x_{i+1}^j]} \left|\frac{\partial^3 s}{\partial x^3}(\eta, t_j)\right| \frac{\varepsilon|h_i^j + h_{i+1}^j|}{3} + \max_{\mu\in[t_{j-1}, t_j]} \left|\frac{\partial^2 s}{\partial t^2}(x_i, \mu)\right| \frac{\Delta t}{2} + CN^{-2+\rho}. \quad (4.34)$$

By using the derivative bounds of s from Theorem 4.1.2 with $h_i^j + h_{i+1}^j \leq CN^{-1}$ and $\sqrt{\varepsilon} \ll N^{-1}$, we get

$$|[L^{N,M}(s-S)]_i^j| \leq CN^{-2} + C\Delta t + CN^{-2+\rho} \leq C(\Delta t + N^{-2+\rho}). \quad (4.35)$$

Now, for the left side boundary, we have

$$\begin{aligned}
[D_0^{N,M}(s-S)]_0^j &= [D_0^{N,M}s]_0^j - \left[\mathcal{D}_0 s(0,t_j) + \frac{h_1^j}{2\sqrt{\varepsilon}}\left(f_0^j - b_0^j(\phi_b)_0^{j-M_\tau}\right)\right] \\
&= s(x_0^j, t_j) - \sqrt{\varepsilon}D_x^+ s(x_0^j, t_j) + \frac{h_1^j}{2\sqrt{\varepsilon}}\left(a_0^j s(x_0^j, t_j) + \delta_t^\star s(x_0^j, t_j)\right) \\
&\quad - \left[s(x_0^j, t_j) - \sqrt{\varepsilon}\frac{\partial s}{\partial x}(x_0^j, t_j) + \frac{h_1^j}{2\sqrt{\varepsilon}}\left(f_0^j - b_0^j(\phi)_0^{j-M_\tau}\right)\right] \\
&= \sqrt{\varepsilon}\left[\frac{\partial s}{\partial x} - D_x^+ s\right](x_0^j, t_j) \\
&\quad + \frac{h_1^j}{2\sqrt{\varepsilon}}\left[-f_0^j + b_0^j(\phi)_0^{j-M_\tau} + a_0^j s(x_0^j, t_j) + \delta_t^\star s(x_0^j, t_j)\right] \\
&= \sqrt{\varepsilon}\left[\frac{\partial s}{\partial x} - \left(D_x^+ s - \frac{h_1^j}{2}\frac{\partial^2 s}{\partial x^2}\right)\right](x_0^j, t_j) + \frac{h_1^j}{2\sqrt{\varepsilon}}\left[\delta_t^\star s - \frac{\partial s}{\partial t}\right](x_0^j, t_j) \\
&= -\frac{\partial^3 s}{\partial x^3}(\eta, t_j)\frac{(h_1^j)^2\sqrt{\varepsilon}}{6} - \frac{\partial^2 s}{\partial t^2}(x_0^j, \mu)\frac{h_1^j \Delta t}{4\sqrt{\varepsilon}},
\end{aligned}$$

for some $\eta \in (x_0^j, x_1^j)$, and $\mu \in (t_{j-1}, t_j)$. Here, interpolation error in the discretization of time derivative is excluded because the interpolation does not make any difference at the boundary points. Using the derivative bounds of s and results in

Lemmas 4.2.2 and 4.2.3, we obtain

$$\begin{aligned} |[D_0^{N,M}(s-S)]_0^j| &\leq \max_{\eta\in[x_0^j,x_1^j]}\left|\frac{\partial^3 s}{\partial x^3}(\eta,t_j)\right|\frac{(h_1^j)^2\sqrt{\varepsilon}}{6} + \max_{\mu\in[t_{j-1},t_j]}\left|\frac{\partial^2 s}{\partial t^2}(x_0^j,\mu)\right|\frac{h_1^j\Delta t}{4\sqrt{\varepsilon}} \\ &\leq C(\Delta t + N^{-2}). \end{aligned} \tag{4.36}$$

Similarly, for the right side boundary, we can obtain

$$|[D_1^{N,M}(s-S)]_0^j| \leq C(\Delta t + N^{-2}). \tag{4.37}$$

Now, we consider the mesh function

$$(\Psi^{\pm})_i^j = C(\Delta t + N^{-2+\rho}) \pm (s(x_i^j,t_j) - S_i^j).$$

From (4.35), we have $L^{N,M}(\Psi^{\pm})_i^j \geq 0$. Further, (4.36) and (4.37) give $D_0^{N,M}(\Psi^{\pm})_0^j \geq 0$ and $D_1^{N,M}(\Psi^{\pm})_N^j \geq 0$, respectively. Thus, using the discrete maximum principle (Lemma 4.2.1) we get

$$|s(x_i^j,t_j) - S_i^j| \leq C(\Delta t + N^{-2+\rho}), \quad \text{for } i = 0,...,N,\ j = 0,...M_\tau. \tag{4.38}$$

Next, to estimate the truncation error for the singular component, we use (4.8) and (4.32) to get

$$|[L^{N,M}(w-W)]_i^j| = -\varepsilon\left(\delta_x^2 - \frac{\partial^2}{\partial x^2}\right)w(x_i^j,t_j) + \left(\delta_t^\star - \frac{\partial}{\partial t}\right)w(x_i^j,t_j).$$

We estimate the error in the singular component according to the location of the mesh points. For outside the layer regions, that is, for $i = \mathcal{S},...,\wp$, Taylor expansion with standard interpolation error estimate and the condition $N^{-\rho} \leq C\Delta t$ for some

$0 < \rho < 1$, lead to

$$|[L^{N,M}(w-W)]_i^j| \leq C\varepsilon \max_{\eta\in[x_{i-1}^j, x_{i+1}^j]} \left|\frac{\partial^2 w}{\partial x^2}(\eta, t_j)\right| + \max_{\mu\in[t_{j-1}, t_j]} \left|\frac{\partial^2 w}{\partial t^2}(x_i^j, \mu)\right| \frac{\Delta t}{2} + CN^{-2+\rho}.$$

Now, using the derivative bounds of w, we have

$$|[L^{N,M}(w-W)]_i^j| \leq C \begin{cases} e^{-\frac{x_{i-1}^j}{\sqrt{\varepsilon}}} + C\Delta t + CN^{-2+\rho}, & x_i^j \leq \frac{1}{2}, \\ e^{-\frac{(1-x_{i+1}^j)}{\sqrt{\varepsilon}}} + C\Delta t + CN^{-2+\rho}, & x_i^j > \frac{1}{2}. \end{cases}$$

When $\mathcal{S} \leq i$ and $x_i^j \leq \frac{1}{2}$,

$$|[L^{N,M}(w-W)]_i^j| \leq C\left(e^{-\frac{x_{\mathcal{S}-1}^j}{2\sqrt{\varepsilon}}}\right)^2 + C\Delta t + CN^{-2+\rho}.$$

Now, from the mesh structure of the equidistributed mesh (Lemma 4.2.2), we have $e^{-\frac{x_{\mathcal{S}-1}^j}{2\sqrt{\varepsilon}}} \leq CN^{-1}$. Therefore, for $\mathcal{S} \leq i$ and $x_i^j \leq \frac{1}{2}$, we obtain

$$|[L^{N,M}(w-W)]_i^j| \leq CN^{-2} + C\Delta t + CN^{-2+\rho} \leq C(\Delta t + N^{-2+\rho}).$$

Again, the same bound can be obtained by using the similar arguments for $i \leq \wp$ and $x_i^j > \frac{1}{2}$.

Next, to estimate the truncation error for $i = 1, ..., \mathcal{S}-1$ and $i = \wp+1, ..., N-1$, we provide the details of the left side boundary layer region as it will be analogous for the right side boundary layer region. Using Taylor expansions, standard interpolation

error estimate and the condition $N^{-\rho} \leq C\Delta t$ for some $0 < \rho < 1$, we get

$$\begin{aligned} |[L^{N,M}(w-W)]_i^j| \;\leq\; & \frac{\varepsilon}{h_i^j + h_{i+1}^j}\left[\max_{\eta\in[x_{i-1}^j, x_{i+1}^j]}\left|\frac{\partial^3 w}{\partial x^3}(\eta, t_j)\right||(h_{i+1}^j)^2 - (h_i^j)^2|\right. \\ & \left. + \max_{\eta\in[x_{i-1}^j, x_{i+1}^j]}\left|\frac{\partial^4 w}{\partial x^4}(\eta, t_j)\right|(h_i^j)^2(h_i^j + h_{i+1}^j)\right] \\ & + \max_{\mu\in[t_{j-1}, t_j]}\left|\frac{\partial^2 w(x_i^j, \mu)}{\partial t^2}\right|\frac{\Delta t}{2} + CN^{-2+\rho}. \end{aligned}$$

Using the derivative bounds of w and Lemmas 4.2.2 and 4.2.3, we get

$$|[L^{N,M}(w-W)]_i^j| \leq C\varepsilon^{-1}(h_i^j)^2 e^{-\frac{x_i^j}{\sqrt{\varepsilon}}} + C\Delta t + CN^{-2+\rho}.$$

Now we can use the equidistribution principle to bound the first term of the left hand side, as follows

$$\begin{aligned} C\varepsilon^{-1}(h_i^j)^2 e^{-\frac{x_i^j}{\sqrt{\varepsilon}}} \;&\leq\; C\varepsilon^{-1}\left(\int_{x_{i-1}^j}^{x_i^j} e^{-\frac{\xi}{2\sqrt{\varepsilon}}}\, d\xi\right)^2 \\ &\leq\; C\varepsilon^{-1}\left(\sqrt{\varepsilon}\int_{x_{i-1}^j}^{x_i^j} \mathcal{M}(y(\gamma), \gamma) d\gamma\right)^2 \leq C\mathbf{K}^2 N^{-2}. \end{aligned}$$

Thus, we have

$$|[L^{N,M}(w-W)]_i^j| \leq C(\Delta t + N^{-2+\rho}). \tag{4.39}$$

For the left side boundary, the truncation error is given by

$$|[D_0^{N,M}(w-W)]_0^j| \leq \max_{\eta\in[x_0^j, x_1^j]}\left|\frac{\partial^3 w}{\partial x^3}(\eta, t_j)\right|\frac{(h_1^j)^2\sqrt{\varepsilon}}{6} + \max_{\mu\in[t_{j-1}, t_j]}\left|\frac{\partial^2 w}{\partial t^2}(x_i^j, \mu)\right|\frac{h_1^j \Delta t}{4\sqrt{\varepsilon}}.$$

Hence, using derivative bounds of w, Lemma 4.2.2 and the equidistribution principle, we get

$$\begin{aligned}
|[D_0^{N,M}(w-W)]_0^j| &\leq C\varepsilon^{-1}(h_1^j)^2 e^{-x_0^j\sqrt{\frac{1}{\varepsilon}}} + C\Delta t \\
&\leq C\varepsilon^{-1}\left(\int_{x_0^j}^{x_1^j} e^{-\frac{\gamma}{2}\sqrt{\frac{1}{\varepsilon}}}d\gamma\right)^2 + C\Delta t \\
&\leq C\varepsilon^{-1}\left(\sqrt{\varepsilon}\int_{x_0^j}^{x_1^j}\mathcal{M}(y(\gamma,t_j),\gamma)d\gamma\right)^2 + C\Delta t \\
&\leq C\mathbf{K}^2N^{-2} + C\Delta t \\
&\leq C(\Delta t + N^{-2}). \qquad (4.40)
\end{aligned}$$

Similarly for the right side boundary we can obtain

$$|[D_1^{N,M}(w-W)]_N^j| \leq C(\Delta t + N^{-2}). \qquad (4.41)$$

Now, we consider the mesh function

$$(\Phi^{\pm})_i^j = C(\Delta t + N^{-2+\rho}) \pm (w(x_i^j,t_j) - W_i^j).$$

From (4.39), we have $L^{N,M}(\Phi^{\pm})_i^j \geq 0$. Further, (4.40) and (4.41) give $D_0^{N,M}(\Phi^{\pm})_0^j \geq 0$ and $D_1^{N,M}(\Phi^{\pm})_N^j \geq 0$, respectively. Thus, using discrete maximum principle in Lemma 4.2.1, we get

$$|w(x_i^j,t_j) - W_i^j| \leq C(\Delta t + N^{-2+\rho}), \quad \text{for } i = 0,...,N,\ j = 0,...,M_\tau. \qquad (4.42)$$

Hence, combining the error bounds of the smooth and singular components from (4.38) and (4.42), for $t_j \in [0,\tau]$, we get

$$|y(x_i^j,t_j) - Y_i^j| \leq C(\Delta t + N^{-2+\rho}), \quad i = 0,...,N. \qquad (4.43)$$

Now, to prove the convergence result for $t_j \in [\tau, 2\tau]$, we consider the discretization of the continuous problem (4.10) as follows

$$L^{N,M}Y_i^j = f_i^j - b_i^j \widetilde{Y}_i^{j-M_\tau}, \quad i = 1, ..., N-1, \ j = M_\tau + 1, ..., 2M_\tau, \tag{4.44}$$

$$\text{with} \quad Y_i^j = Y_i^j, \quad i = 0, ..., N, \ j = 1, ..., M_\tau,$$

$$\text{and} \quad \begin{cases} D_0^{N,M}Y_0^j = (\phi_0)(t_j) + \frac{h_1^j}{2\sqrt{\varepsilon}}\left(f_0^j - b_0^j \widetilde{Y}_0^{j-M_\tau}\right), & j = M_\tau + 1, ..., 2M_\tau, \\ D_1^{N,M}Y_N^j = (\phi_1)(t_j) + \frac{h_N^j}{2\sqrt{\varepsilon}}\left(f_N^j - b_N^j \widetilde{Y}_N^{j-M_\tau}\right), & j = M_\tau + 1, ..., 2M_\tau. \end{cases}$$

Again, we consider the decomposition of discrete solution Y as $Y = S + W$, where S is the solution of the following discrete problem

$$L^{N,M}S_i^j = f_i^j - b_i^j \widetilde{S}_i^{j-M_\tau}, \quad i = 1, ..., N-1, \ j = M_\tau + 1, ..., 2M_\tau, \tag{4.45}$$

$$\text{with} \quad S_i^j = Y_i^j, \quad i = 0, ..., N, \ j = 1, ...M_\tau,$$

$$\text{and} \quad \begin{cases} D_0^{N,M}S_0^j = \mathcal{D}_0 s(0, t_j) + \frac{h_1^j}{2\sqrt{\varepsilon}}\left(f_0^j - b_0^j \widetilde{S}_0^{j-M_\tau}\right), & j = M_\tau + 1, ..., 2M_\tau, \\ D_1^{N,M}S_N^j = \mathcal{D}_1 s(1, t_j) + \frac{h_N^j}{2\sqrt{\varepsilon}}\left(f_N^j - b_N^j \widetilde{S}_N^{j-M_\tau}\right), & j = M_\tau + 1, ..., 2M_\tau, \end{cases}$$

and W satisfies

$$L^{N,M}W_i^j = -b_i^j \widetilde{W}_i^{j-M_\tau}, \quad i = 1, ..., N-1, \ j = M_\tau + 1, ..., 2M_\tau, \tag{4.46}$$

$$\text{with} \quad W_i^j = 0, \quad i = 0, ..., N, \ j = 1, ...M_\tau,$$

$$\text{and} \quad \begin{cases} D_0^{N,M}W_0^j = \phi_0(t_j) - \mathcal{D}_0 s(0, t_j) + \frac{h_1^j}{2\sqrt{\varepsilon}}\left(-b_0^j \widetilde{W}_0^{j-M_\tau}\right), & j = M_\tau + 1, ..., 2M_\tau, \\ D_1^{N,M}W_N^j = \phi_1(t_j) - \mathcal{D}_1 s(1, t_j) + \frac{h_N^j}{2\sqrt{\varepsilon}}\left(-b_N^j \widetilde{W}_N^{j-M_\tau}\right), & j = M_\tau + 1, ..., 2M_\tau. \end{cases}$$

Thus, the error can be decomposed as

$$|y - Y| = |s - S| + |w - W|. \tag{4.47}$$

For the smooth component s, we have

$$[L^{N,M}(s-S)]_i^j = -b_i^j\left(s(x_i^j,t_{j-M_\tau}) - \widetilde{S}_i^{j-M_\tau}\right) - \varepsilon\left(\delta_x^2 - \frac{\partial^2}{\partial x^2}\right)s(x_i^j,t_j) + \left(\delta_t^\star - \frac{\partial}{\partial t}\right)s(x_i^j,t_j).$$

The first term can be bounded using (4.38) and standard interpolation error bounds. The other terms can be bounded by using the previous arguments as in (4.35)). Thus, we obtain

$$|[L^{N,M}(s-S)]_i^j| \leq C(\Delta t + CN^{-2+\rho}). \tag{4.48}$$

At the boundaries, we again use the previous arguments to get

$$|[D_0^{N,M}(s-S)]_0^j| \leq C(\Delta t + N^{-2}) \tag{4.49}$$

and

$$|[D_1^{N,M}(s-S)]_N^j| \leq C(\Delta t + N^{-2}),\ t_j \in (\tau, 2\tau]. \tag{4.50}$$

Now, considering $(\Psi^\pm)_i^j = C(\Delta t + N^{-2+\rho}) \pm (s(x_i^j,t_j) - S_i^j)$, (4.48) gives $L^{N,M}(\Psi^\pm)_i^j \geq 0$, and (4.49), (4.50) give $D_0^{N,M}(\Psi^\pm)_0^j \geq 0$ and $D_1^{N,M}(\Psi^\pm)_N^j \geq 0$, respectively. Thus, using discrete maximum principle (Lemma 4.2.1), we get

$$|s(x_i,t_j) - S_i^j| \leq C(\Delta t + N^{-2+\rho}), \quad \text{for } i = 0,...,N,\ j = M_\tau,...,2M_\tau. \tag{4.51}$$

Next, to estimate the truncation error for the singular component, we have from (4.13) and (4.46),

$$|[L^{N,M}(w-W)]_i^j| = -b_i^j\left(w(x_i^j,t_{j-M_\tau}) - \widetilde{W}_i^{j-M_\tau}\right) - \varepsilon\left(\delta_x^2 - \frac{\partial^2}{\partial x^2}\right)w(x_i^j,t_j) + \left(\delta_t^\star - \frac{\partial}{\partial t}\right)w(x_i^j,t_j).$$

The first term can be bounded using standard interpolation error bounds and (4.42). Using arguments similar for $t_j \in [0,\tau]$, we get the following estimate for $t_j \in (\tau, 2\tau]$:

$$\left|[L^{N,M}(W-w)]_i^j\right| \leq C(\Delta t + N^{-2+\rho}). \tag{4.52}$$

Again for the boundaries, we use previous arguments to get

$$|[D_0^{N,M}(w-W)]_0^j| \leq C(\Delta t + N^{-2+\rho}) \tag{4.53}$$

and

$$|[D_1^{N,M}(w-W)]_N^j| \leq C(\Delta t + N^{-2+\rho}), t_j \in (\tau, 2\tau]. \tag{4.54}$$

Now, considering $(\Phi^{\pm})_i^j = C(\Delta t + N^{-2+\rho}) \pm (w(x_i^j,t_j) - W_i^j)$, (4.52) gives $L^{N,M}(\Phi^{\pm})_i^j \geq 0$, and (4.53), (4.54) give $D_0^{N,M}(\Phi^{\pm})_0^j \geq 0$ and $D_1^{N,M}(\Phi^{\pm})_N^j \geq 0$, respectively. Now, using discrete maximum principle (Lemma 4.2.1), we get

$$|w(x_i,t_j) - W_i^j| \leq C(\Delta t + N^{-2+\rho}), \quad \text{for } i = 0,...,N,\ j = M_\tau,...,2M_\tau. \tag{4.55}$$

Therefore, combining the error bounds in (4.51) and (4.55), we get

$$|y(x_i,t_j) - Y_i^j| \leq C(\Delta t + N^{-2+\rho}), \quad \text{for } i = 0,...,N,\ j = M_\tau,...,2M_\tau. \tag{4.56}$$

Hence, the result follows by using mathematical induction. □

Remark 4.3.1. We want to note that the assumption $N^{-\rho} \leq C\Delta t$, for some $0 < \rho < 1$, in the above theorem, does not have any influence in the convergence behavior of the numerical solution, which can be seen in the next section.

4.4 Numerical experiments

Now, we provide strong numerical evidences in favor of our theoretical findings. We use the following moving mesh algorithm to construct the equidistributed mesh and the boundary layer-adaptive solution on this mesh. This algorithm is originally proposed by de Boor [47] and has been also used by several researchers, for example [58, 61, 62, 71, 115]. The convergence analysis of de Boor algorithm is discussed in [116]. In practice, we can write the discrete version of the equidistribution problem as

$$h_i^k \mathcal{M}_i^k = \frac{1}{N} \sum_{i=1}^{N} h_i^k \mathcal{M}_i^k, \ i = 1, ..., N, \tag{4.57}$$

where $\mathcal{M}_i^k$ is the discrete approximation of $\mathcal{M}(x_i^k, t_k)$. However, for the numerical experiments, we need to reformulate (4.57) into the following weakened form of the equidistribution principle

$$h_i^k \mathcal{M}_i^k \leq \frac{\varrho}{N} \sum_{i=1}^{N} h_i^k \mathcal{M}_i^k, \ i = 1, ..., N. \tag{4.58}$$

Here, $\varrho > 1$ is a user chosen constant. If we choose ϱ near to 1, the obtained solution will be more accurate and correspondingly, the number of iteration will become larger. In our numerical experiments, we have taken $\varrho = 1.1$. Note that, the second order derivative of regular component of the solution is uniformly bounded from (4.16). Hence, it will be appropriate to use Y in place of the layer component W in (4.24) (see also [124]).

Algorithm 3: Algorithm for the adaptive mesh and adaptive solution

Input: $N,\ M \in \mathbb{N},\ 0 < \varepsilon \leq 1$ and $\varrho > 1$.

Output: Adaptive mesh $\{x_i^k\}$ and adaptive solution Y_i^m at each time level t_m.

1. Take uniform mesh in each sub-interval $[0,\tau],[\tau,2\tau],\cdots,[(m-1)\tau,T]$ (of the time domain) containing exactly M_τ mesh partitions at every subinterval. Initialize (iteration $r=1$) the spatial mesh $\{x_i^{k,(r)}\}$ as the uniform mesh at time level $t_k = t_1$. Now we show the procedure for obtaining solution at $[0,\tau]$.

2. Solve the discrete problem (4.19) for $Y_i^{k,(r)}$ on $\{x_i^{k,(r)}\}$ using linear interpolants of Y_i^{k-1} and $Y_i^{k-M_\tau}$ on the mesh $\{x_i^{k,(r)}\}$. Here the delayed solution will be used.

3. Find the discrete monitor function, defined by

$$\mathcal{M}_i^{k,(r)} = \aleph^{k,(r)} + |\delta_x^2 Y_i^{k,(r)}|^{1/2}, \quad \text{for } i = 1,...,N-1,$$

where $\aleph^{k,(r)}$ is defined by

$$\aleph^{k,(r)} = h_1^{k,(r)}|\delta_x^2 Y_1^{k,(r)}|^{1/2} + \sum_{i=2}^{N-1} h_i^{k,(r)} \left\{ \frac{|\delta_x^2 Y_{i-1}^{k,(r)}|^{1/2} + |\delta_x^2 Y_i^{k,(r)}|^{1/2}}{2} \right\} + h_N^{k,(r)}|\delta_x^2 Y_{N-1}^{k,(r)}|^{1/2}.$$

4. Set $H_i^{k,(r)} = h_i^{k,(r)}\left(\frac{\mathcal{M}_{i-1}^{k,(r)} + \mathcal{M}_i^{k,(r)}}{2}\right)$ for $i = 1,...,N$, take $\mathcal{M}_0^{k,(r)} = \mathcal{M}_1^{k,(r)}$ and $\mathcal{M}_N^{k,(r)} = \mathcal{M}_{N-1}^{k,(r)}$. Then, define $A_i^{k,(r)}$ by$A_i^{k,(r)} = \sum_{j=1}^{i} H_j^{k,(r)}$ for $i = 1,...,N$ and $A_0^{k,(r)} = 0$.

5. **Stopping criterion**: Define $\varrho^{(r)}$ by $\varrho^{(r)} = \frac{N}{A_N^{k,(r)}} \max\limits_{i=1,...,N} H_i^{k,(r)}$. Go to Step 7, if $\varrho^{(r)} \leq \varrho$, else continue with Step 6.

6. Define $Q_i^{k,(r)} = i\frac{A_N^{k,(r)}}{N}$ for $i = 0,...,N$. New mesh $\{x_i^{k,(r+1)}\}$ is generated by evaluating the interpolation of the points $(A_i^{k,(r)}, x_i^{k,(r)})$ at $Q_i^{k,(r)}$. Set $r = r+1$ and return to Step 2.

7. Take $\{x_i^{k,*}\} = \{x_i^{k,(r)}\}$ as the final layer-adaptive mesh at $t = t_k$; and $Y_i^{k,*} = Y_i^{k,(r)}$ as the required adaptive solution at this time.

8. Go to Step 2 with $k = k+1$, to find the numerical solution at next time level with $\{x_i^k\}$ as the initial iteration for time level t_{k+1}. Repeat the process, till we reach the endpoint $t = \tau$ of the first time subinterval $[0,\tau]$.

9. Now use the same procedure to find the adaptive solution at every time subinterval $[\tau,2\tau],\cdots,[(m-1)\tau,T]$ till the final time is reached, by repeating the procedures from Step 2 (say with the time $t = \tau$ for the time subinterval $[\tau,2\tau]$), and $r = 1$.

Numerical Examples

Example 4.4.1. Let us consider the following time delayed Robin type boundary value problem:

$$\frac{\partial y}{\partial t} - \varepsilon \frac{\partial^2 y}{\partial x^2} + (1 + xe^{-t})y = f(x,t) - y(x,t-1), \quad (x,t) \in (0,1) \times (0,2],$$

$$\text{with} \quad y(x,t) = \phi_b(x,t), \ (x,t) \in [0,1] \times [-1,0],$$

$$\text{and} \quad \begin{cases} \mathcal{D}_0 y(0,t) = \phi_0(t), \ t \in (0,2], \\ \mathcal{D}_1 y(1,t) = \phi_1(t), \ t \in (0,2], \end{cases}$$

where the functions $f(x,t)$, $\phi_0(t)$, $\phi_1(t)$ and $\phi_b(x,t)$ are chosen to satisfy the exact solution

$$y(x,t) = t\left(\frac{e^{-x/\sqrt{\varepsilon}} + e^{-(1-x)/\sqrt{\varepsilon}}}{1 + e^{-1/\sqrt{\varepsilon}}} - \cos^2(\pi x)\right).$$

Figure 4.1 displays the solution plot of Example 4.4.1 for $\varepsilon = 10^{-6}$ with $N = 64$ and $M = 32$. The presence of boundary layers at $x = 0$ and $x = 1$, can be clearly confirmed from this figure. In addition, Figure 4.2 shows that the initial uniform mesh points have moved to the boundary layer regions based on the above iterative moving mesh algorithm, and the equidistributed mesh is also dense to the boundary regions for Example 4.4.1. Now, we calculate the maximum pointwise errors and rates of convergence for different values of ε and discretization parameters M and N by using the following formulas

$$E^{\varepsilon,N,M} = \max_{i,k} |Y_i^k - y(x_i^k, t_k)|, \qquad F^{\varepsilon,N,M} = \log_2\left(\frac{E^{\varepsilon,N,M}}{E^{\varepsilon,2N,2M}}\right).$$

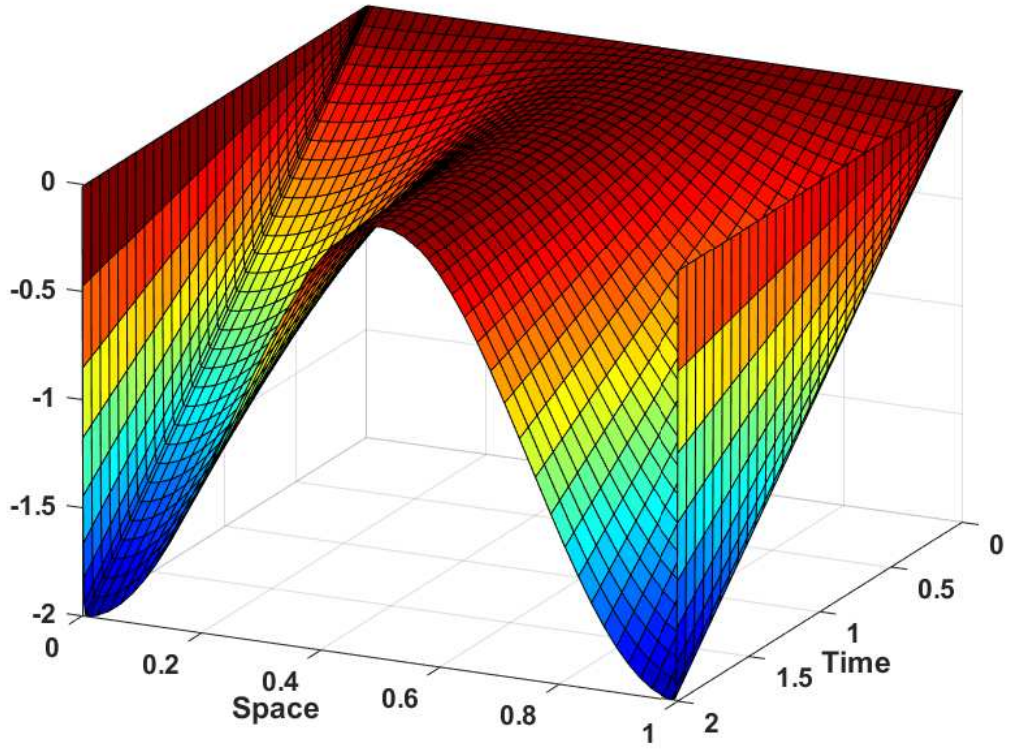

FIGURE 4.1: Boundary layer-adapted numerical soluton of Example 4.4.1 with $N = 64,\ M = 32$ and $\varepsilon = 10^{-6}$.

The parameter-robust errors and the corresponding rates of convergence are calculated by

$$E^{N,M} = \max_{\varepsilon} E^{\varepsilon,N,M}, \qquad F^{N,M} = \log_2 \left(\frac{E^{N,M}}{E^{2N,2M}} \right),$$

respectively.

Table 4.1 represents the parameter-robust convergence for Example 4.4.1. The overall second order accuracy in space and time, is due to the fact that the present problem is space dominated for the input data given in Table 4.1. The expected rate of accuracy for a general problem, which matches with theoretical findings, will be clear from Example 4.4.2.

Further, we give a comparison of uniform accuracy between the proposed approach

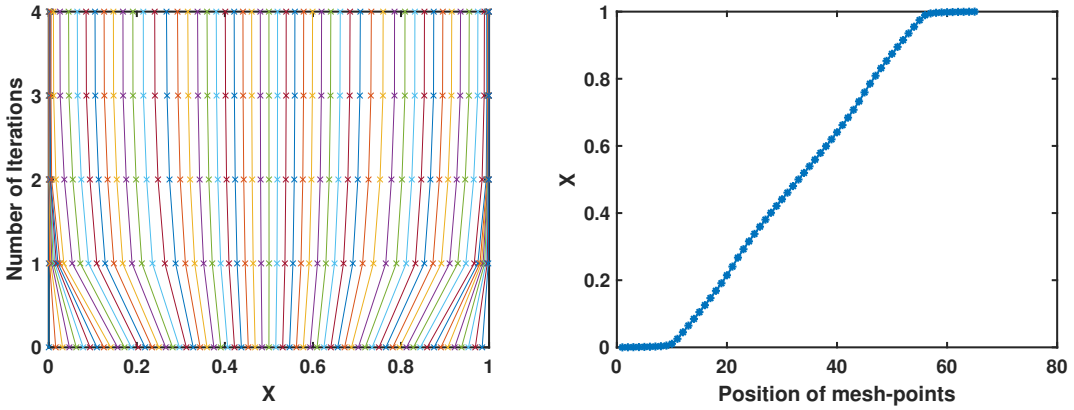

(a) Moving mesh trajectory (b) Density of spatial mesh

FIGURE 4.2: Iteration-wise moving mesh trajectory and mesh density in space at final time resp., for $N = 64$, $M = 32$ and $\varepsilon = 10^{-6}$ of Example 4.4.1.

on equidistributed mesh with the approximate solution, obtained on existed Shishkin mesh in Table 4.2 for Example 4.4.1. The Shishkin mesh is defined using the transition parameter $\sigma = \min\{1/4, 2\sqrt{\varepsilon}\ln(N)\}$. It clearly shows that, the numerical solution obtained on a Shishkin mesh, is lesser accurate compared to the present approach. This is also expected from our theoretical findings, as the order of accuracy of approximate solution on Shishkin mesh is at most $O(N^{-2}\ln^2(N))$ in space, for the present scheme. Also, note that the errors at equidistributed mesh is far less compared to errors on Shishkin mesh irrespective of the perturbation parameters.

Example 4.4.2. Now, let us consider the time delayed parabolic PDE with Robin type boundary conditions:

$$\frac{\partial y}{\partial t} - \varepsilon\frac{\partial^2 y}{\partial x^2} + \frac{1+x^2}{2}y = t^3 - y(x, t-1), \quad (x,t) \in (0,1)\times(0,2],$$

$$\text{with} \quad y(x,t) = 0, \ (x,t) \in [0,1]\times[-1,0],$$

$$\text{and} \quad \begin{cases} \mathcal{D}_0 y(0,t) = -\frac{128}{35}\pi^{-1/2}t^{7/2}, \ t \in (0,2], \\ \mathcal{D}_1 y(1,t) = -\frac{128}{35}\pi^{-1/2}t^{7/2}, \ t \in (0,2]. \end{cases}$$

TABLE 4.1: Maximum pointwise errors $E^{\varepsilon,N,M}$, parameter-robust errors $E^{N,M}$, rates of convergence $F^{\varepsilon,N,M}$ and parameter-robust convergence rates $F^{N,M}$ using scheme (4.19) for Example 4.4.1.

ε	$N=32$ $\Delta t=1/8$	$N=64$ $\Delta t=1/16$	$N=128$ $\Delta t=1/32$	$N=256$ $\Delta t=1/64$	$N=512$ $\Delta t=1/128$	$N=1024$ $\Delta t=1/256$
10^{-1}	3.3229e-03	8.5091e-04	2.1776e-04	5.4424e-05	1.3610e-05	3.4041e-06
	1.9654	1.9662	2.0004	1.9996	1.9993	
10^{-2}	5.7689e-03	1.4149e-03	3.5227e-04	8.7940e-05	2.1981e-05	5.4947e-06
	2.0276	2.0059	2.0021	2.0003	2.0001	
10^{-3}	1.7627e-02	4.5435e-03	1.0607e-03	2.5933e-04	6.4431e-05	1.6081e-05
	1.9559	2.0988	2.0322	2.0090	2.0024	
10^{-4}	3.1762e-02	7.3546e-03	1.7625e-03	4.3722e-04	1.1139e-04	2.7438e-05
	2.1106	2.0610	2.0112	1.9728	2.0213	
10^{-5}	4.4253e-02	9.3469e-03	2.2562e-03	5.5237e-04	1.3756e-04	3.4357e-05
	2.2432	2.0506	2.0302	2.0056	2.0014	
10^{-6}	5.4466e-02	1.0587e-02	2.4723e-03	6.0734e-04	1.5054e-04	3.7571e-05
	2.3631	2.0983	2.0253	2.0123	2.0025	
10^{-7}	6.3989e-02	1.1225e-02	2.5919e-03	6.3013e-04	1.5585e-04	3.8828e-05
	2.5111	2.1147	2.0403	2.0155	2.0050	
10^{-8}	6.7095e-02	1.2316e-02	2.6467e-03	6.4081e-04	1.5801e-04	3.9357e-05
	2.4456	2.2183	2.0462	2.0199	2.0053	
$E^{N,M}$	6.7095e-02	1.2316e-02	2.6467e-03	6.4081e-04	1.5801e-04	3.9357e-05
$F^{N,M}$	2.4456	2.2183	2.0462	2.0199	2.0053	

TABLE 4.2: Comparison of parameter-robust errors $E^{N,M}$ and corresponding convergence rates $F^{N,M}$ obtained on Shishkin and equidistribution meshes using scheme (4.19) for Example 4.4.1.

$\varepsilon \in \mathcal{E}_\varepsilon$	$N=32$ $\Delta t=1/8$	$N=64$ $\Delta t=1/16$	$N=128$ $\Delta t=1/32$	$N=256$ $\Delta t=1/64$	$N=512$ $\Delta t=1/128$	$N=1024$ $\Delta t=1/256$
Shishkin mesh [98]	7.0933e-02	2.8034e-02	9.9156e-03	3.2837e-03	1.0439e-03	3.2271e-04
	1.3393	1.4994	1.5944	1.6533	1.6938	
Equidistribution mesh	6.7095e-02	1.2316e-02	2.6467e-03	6.4081e-04	1.5801e-04	3.9357e-05
	2.4456	2.2183	2.0462	2.0199	2.0053	

The exact solution of this example is unknown. Hence, we use a variant of the double mesh principle [58, 113] to compute the pointwise errors and corresponding rates of convergence. Based on this principle, the numerical solution on equidistributed mesh will be compared with the solution, which is obtained on the bisected equidistributed

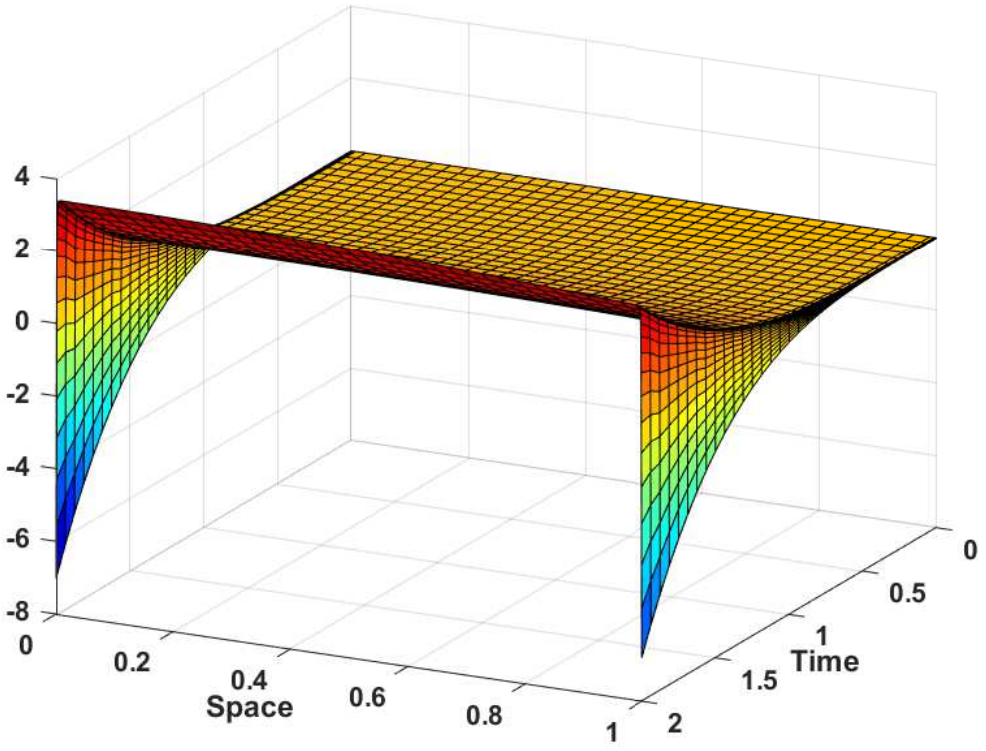

FIGURE 4.3: Boundary layer-adapted numerical solution of Example 4.4.2 with $N = 64,\ M = 32$ and $\varepsilon = 10^{-6}$.

mesh. The error and rate of convergence formulae based on this technique are

$$E^{\varepsilon,N,M} = \max_{i,k} |Y_i^{k,2N,2M} - Y_i^{k,N,M}|, \qquad F^{\varepsilon,N,M} = \log_2 \left(\frac{E^{\varepsilon,N,M}}{E_\varepsilon^{2N,2M}} \right).$$

The uniform errors and corresponding rates of convergence are calculated as before.

As like in Example 4.4.1, one can also observe the boundary layer phenomena for Example 4.4.2 from Figure 4.3, which is plotted with a very small perturbation parameter $\varepsilon = 10^{-6}$. Here, note that the present method with discretized Robin boundary condition, is first order uniform accurate in space and time from Table 4.3. This is matching with our theoretical findings. This also shows the dominant

TABLE 4.3: Maximum pointwise errors $E^{\varepsilon,N,M}$, parameter-robust errors $E^{N,M}$, rates of convergence $F^{\varepsilon,N,M}$ and parameter-robust convergence rates $F^{N,M}$ using scheme (4.19) for Example 4.4.2.

	$N=32$	$N=64$	$N=128$	$N=256$	$N=512$	$N=1024$
ε	$\Delta t=1/8$	$\Delta t=1/16$	$\Delta t=1/32$	$\Delta t=1/64$	$\Delta t=1/128$	$\Delta t=1/256$
10^{-1}	6.0082e-02	3.0886e-02	1.5975e-02	8.1454e-03	4.1073e-03	2.0650e-03
	0.9600	0.9511	0.9718	0.9878	0.9921	
10^{-2}	1.2543e-01	6.3953e-02	3.2216e-02	1.6183e-02	8.1117e-03	4.0604e-03
	0.9718	0.9892	0.9933	0.9964	0.9984	
10^{-3}	1.3828e-01	6.9972e-02	3.5175e-02	1.7642e-02	8.8342e-03	4.4210e-03
	0.9827	0.9922	0.9956	0.9978	0.9987	
10^{-4}	1.4091e-01	7.1091e-02	3.5705e-02	1.7892e-02	8.9564e-03	4.4807e-03
	0.9870	0.9936	0.9968	0.9983	0.9992	
10^{-5}	1.4139e-01	7.1290e-02	3.5793e-02	1.7934e-02	8.9762e-03	4.4903e-03
	0.9879	0.9940	0.9970	0.9985	0.9993	
10^{-6}	1.4152e-01	7.1340e-02	3.5813e-02	1.7941e-02	8.9790e-03	4.4916e-03
	0.9882	0.9942	0.9973	0.9986	0.9993	
10^{-7}	1.4152e-01	7.1357e-02	3.5817e-02	1.7943e-02	8.9798e-03	4.4919e-03
	0.9879	0.9944	0.9973	0.9986	0.9994	
10^{-8}	1.4988e-01	7.1365e-02	3.5818e-02	1.7944e-02	8.9798e-03	4.4919e-03
	1.0705	0.9945	0.9972	0.9987	0.9994	
$E^{N,M}$	1.4988e-01	7.1365e-02	3.5818e-02	1.7944e-02	8.9798e-03	4.4919e-03
$F^{N,M}$	1.0705	0.9945	0.9972	0.9987	0.9994	

behavior of the time discretization error over space errors when we compute the global errors.

To show the global first order accuracy is due to time in Table 4.3, we balance the contribution of time and space discretizations by making the number of mesh points double in space and quadruple in time. That is,

$$\hat{F}^{\varepsilon,N,M} = \log_2\left(\frac{E^{\varepsilon,N,M}}{E^{\varepsilon,2N,4M}}\right), \qquad \hat{F}^{N,M} = \log_2\left(\frac{E^{N,M}}{E^{2N,4M}}\right).$$

Based on this formulae, Table 4.4 shows the second order parameter-robust accuracy. This means that the rate of space accuracy, is two. This can also be confirmed from the log-log plots of the maximum pointwise errors in Figure 4.4. In addition, a comparison of the proposed method on equidistributed meshes with the result on

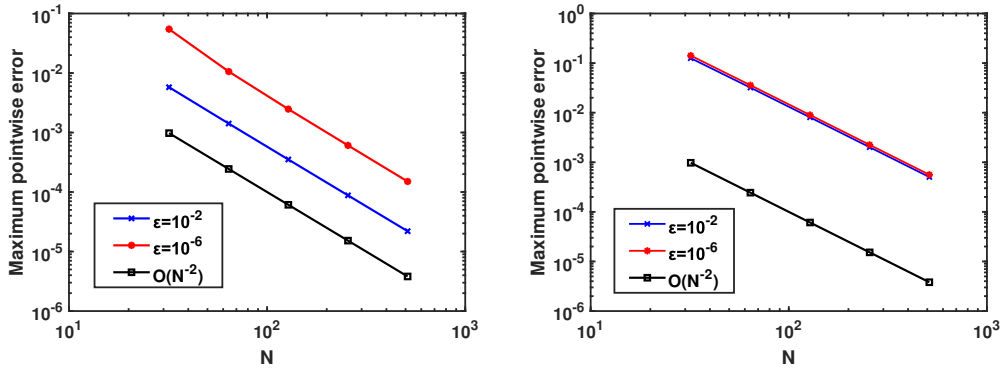

(a) For Example 4.4.1 (b) For Example 4.4.2

FIGURE 4.4: Log-log plots for order of convergence of error vs N.

TABLE 4.4: Maximum pointwise errors $E^{\varepsilon,N,M}$, parameter-robust errors $E^{N,M}$, rates of convergence $F^{\varepsilon,N,M}$ and parameter-robust convergence rates $F^{N,M}$ using scheme (4.19) for Example 4.4.2.

	$N=32$	$N=64$	$N=128$	$N=256$	$N=512$	$N=1024$
ε	$\Delta t=1/8$	$\Delta t=1/32$	$\Delta t=1/128$	$\Delta t=1/512$	$\Delta t=1/2048$	$\Delta t=1/8192$
10^{-1}	6.0082e-02	1.4588e-02	3.6751e-03	9.4177e-04	2.3091e-04	5.7627e-05
	2.0422	1.9889	1.9644	2.0281	2.0025	
10^{-2}	1.2543e-01	3.2020e-02	8.0533e-03	2.0131e-03	5.0410e-04	1.2613e-04
	1.9698	1.9913	2.0002	1.9976	1.9988	
10^{-3}	1.3828e-01	3.5060e-02	8.8002e-03	2.2004e-03	5.4968e-04	1.3744e-04
	1.9797	1.9942	1.9997	2.0011	1.9998	
10^{-4}	1.4091e-01	3.5676e-02	8.9445e-03	2.2378e-03	5.5923e-04	1.3958e-04
	1.9817	1.9959	1.9989	2.0006	2.0023	
10^{-5}	1.4139e-01	3.5766e-02	8.9699e-03	2.2438e-03	5.6076e-04	1.4001e-04
	1.9830	1.9954	1.9991	2.0005	2.0019	
10^{-6}	1.4152e-01	3.5804e-02	8.9743e-03	2.2446e-03	5.6087e-04	1.4005e-04
	1.9828	1.9962	1.9994	2.0007	2.0017	
10^{-7}	1.4152e-01	3.5813e-02	8.9773e-03	2.2967e-03	5.6096e-04	1.4676e-04
	1.9825	1.9961	1.9667	2.0336	1.9344	
10^{-8}	1.4988e-01	3.5801e-02	8.9782e-03	2.2455e-03	5.6084e-04	1.8090e-04
	2.0657	1.9955	1.9994	2.0014	1.6324	
$E^{N,M}$	1.4988e-01	3.5813e-02	8.9782e-03	2.2967e-03	5.6096e-04	1.8090e-04
$F^{N,M}$	2.0653	1.9960	1.9669	2.0336	1.6327	

Shishkin mesh is also provided in Table 4.5 which clearly gives the benifit of the proposed approach.

Further, we can visualize the mesh movement towards the boundary layers, based

TABLE 4.5: Comparison of parameter-robust errors $E^{N,M}$ and corresponding convergence rates $F^{N,M}$ obtained on Shishkin and equidistribution meshes using scheme (4.19) for Example 4.4.2.

	$N = 32$	$N = 64$	$N = 128$	$N = 256$	$N = 512$	$N = 1024$
$\varepsilon \in \mathcal{E}_\varepsilon$	$\Delta t = 1/8$	$\Delta t = 1/32$	$\Delta t = 1/128$	$\Delta t = 1/512$	$\Delta t = 1/2048$	$\Delta t = 1/8192$
Shishkin	8.3543e-01	3.7914e-01	1.4170e-01	4.7917e-02	1.5362e-02	4.7667e-03
mesh [98]	1.1398	1.4200	1.5642	1.6412	1.6883	
Equidistribution	1.4988e-01	3.5813e-02	8.9782e-03	2.2967e-03	5.6096e-04	1.8090e-04
mesh	2.0653	1.9960	1.9669	2.0336	1.6327	

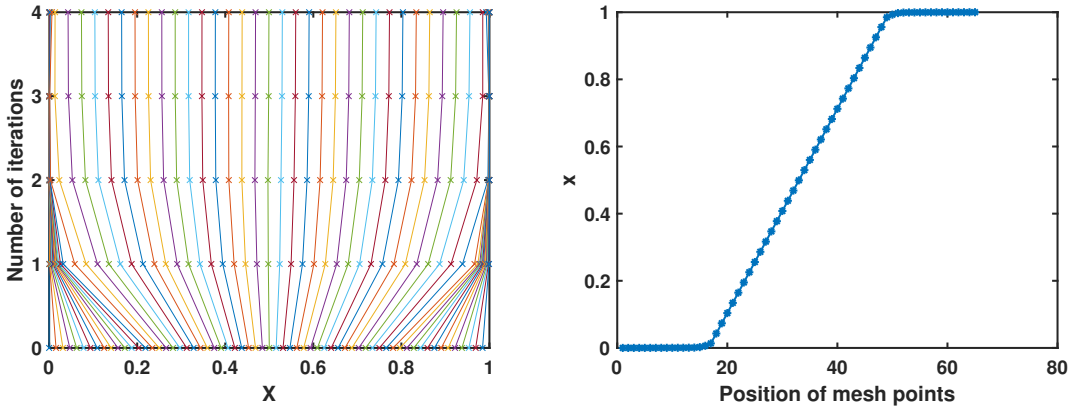

(a) Moving mesh trajectory (b) Density of spatial mesh

FIGURE 4.5: Iteration-wise moving mesh trajectory and mesh density in space at final time, resp., for $N = 64$, $M = 32$ and $\varepsilon = 10^{-6}$ of Example 4.4.2.

on moving mesh algorithm by Figure 4.5. It shows the mesh trajectory at each iteration to generate a layer-adaptive equidistributed mesh. This also pictorially point out that the classical uniform mesh is not sufficient for any general class of Robin type time delayed singularly perturbed problems with arbitrary small perturbation parameters.

4.5 Conclusions

We have proposed a higher order parameter-robust approximation in space for a class of singularly perturbed time delayed parabolic reaction-diffusion problem with Robin boundary conditions. This is not obvious with classical upwind schemes (like

forward-backward discretization at boundary conditions) for problems with Robin type boundary conditions. It is observed that equidistribution based adaptive mesh is very effective for this purpose, as it keeps the optimal accuracy in space, in the interior part of the domain. Theoretical findings of first order uniform accuracy in time and second order uniform accuracy in space, are strongly confirmed experimentally. The present direction on higher order scheme generations for a general system of parabolic problems, will be helpful for next generation researchers working on Robin/mixed type problems.

****